

Stiffness analysis of the sarafix external fixator of composite materials

NedimPervan*, ElmedinMesic, Mirsad Colic, VahidAvdic

University of Sarajevo, Faculty of Mechanical Engineering, B&H

*Corresponding author E-mail: pervan@mef.unsa.ba

Abstract

This paper describes a structural analysis of the CAD model three versions fixators Sarafix which to explore the possibility of introducing composite materials in the construction of the connecting rod fixators comparing values of displacement and stiffness at characteristic points structure. Namely, we investigated constructional performance of fixators Sarafix with a connecting rod formed from three different composite materials, the same matrix (epoxy resin) with three different types of fibers (E glass, kevlar 49 and carbon M55J). Results of structural analysis fixators Sarafix with a connecting rod made of composite materials are compared with the results of tubular connecting rod fixators made of stainless steel. After comparing the results, from the aspect of stiffness, we gave the final considerations about composite material which provides an adequate substitution for the existing material.

Keywords: Composite Materials; External Fixation; Stiffness; Structural Analysis.

1. Introduction

External fixator systems are medical devices for stabilization of bone fractures, and their compliance aims at producing an inter-fragmentary motion that promotes rapid and successful healing. The aim of the fixation technique is anatomical reduction and immobilization of the bone segments, as well as maintenance of this anatomical stabilization concept throughout the treatment by external stiffening of the fracture gap separating the bone segments.

This aim is achieved by an external frame that is connected percutaneously to the bone segments by pins or wires.

Sarafix external fixation system represents a unilateral, biplanar external fixator which belongs to a group of modular fixators with one-half pins (Figure 1).

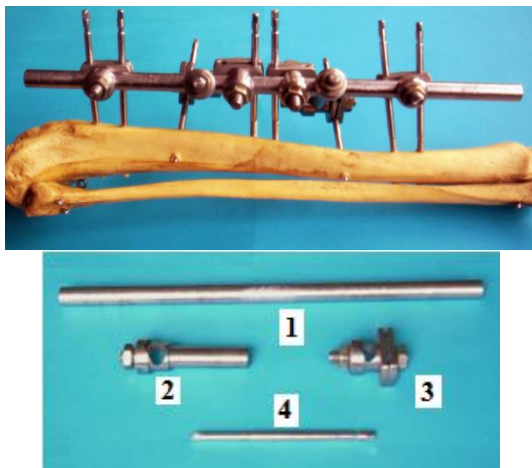


Fig. 1: Sarafix Fixator (Configuration C50) and Fixator Components (1 - Connecting Rod, 2 - Carrier Connector, 3 - Connector, 4 - Half-Pin).

Owing to the high flexibility and mobility, its application is possible to the complete human skeleton. Sarafix is the holder of numerous awards and prizes at international exhibitions of innovations, and gold medals at the exhibitions of innovations Brussels Eureka 95 and Geneva 1996, and Sarajevo's Sixth of April Award for 2001 should be emphasized.

The materials used for making fixator Sarafix are standard stainless steels. Namely, now in orthopedic surgery for making fixator are used primarily stainless steels, superalloys based on cobalt, titanium and its alloys, and less frequently composite materials. The aim of this paper is to develop a CAD model and structural analysis external fixation system of composite materials, which should show the positive and negative effects of the introduction of composite materials in the fixator Sarafix.

2. Composite materials in structural analysis of fixator sarafix

During the testing of fixator Sarafix, composite materials will be applied to the connecting rod of fixators. Composite materials which will be used, consists of a combination of epoxy resin and three types of fibers. Depending on the type of the applied material on the connecting rod, will be formed three versions of fixator Sarafix, namely:

- E50 (E glass / epoxy resin),
- K50 (kevlar 49 / epoxy resin),
- F50 (carbon M55J / epoxy resin).

During the analysis of results, will be used the results from the literature [1], ie. the results for the C50 configuration. The difference between the tested configuration and configuration C50 is a material that is applied to the connecting rod of fixator.

The problem that arises in the selection of composite materials is a guarantee of their quality, and mechanical properties. Almost all the manufacturers and distributors of composite materials, proper-

ties of composite materials provide as approximate [9]. Mechanical properties of composite materials used in the tests are given in table 1.

Table 1: Mechanical Properties of Composite Materials [2],[9]:

	Symbol	Materials			
		E glass / epoxy	Kevlar49 / epoxy	Carbon M55J / epoxy	X30Cr13
Normal Young Modulus	E11 , Ex, ER	20 GPa	70 GPa	230 GPa	
Transverse Young Modulus	E22 , Ey, ET	25 GPa	65 GPa	250 GPa	215GPa
Longitudinal Young Modulus	E33, Ez, EL	30 GPa	60 GPa	270 GPa	
Poisson Ratio in XY plane	ν_{12} , ν_{RT} , $\nu_{x'y'}$	0,2	0,2	0,3	
Poisson Ratio in XZ plane	ν_{13} , ν_{RL} , $\nu_{x'z'}$	0,166	0,17	0,27	0,29
Poisson Ratio in YZ plane	ν_{23} , ν_{TL} , $\nu_{y'z'}$	0,133	0,14	0,2	
ShearModulus in XY plane	G12, GRT, $G_{x'y'}$	5 GPa	5 GPa	6 GPa	
ShearModulus in XZ plane	G13, GRL, $G_{x'z'}$	4 GPa	4 GPa	5 GPa	83 GPa
ShearModulus in YZ plane	G23, GTL, $G_{y'z'}$	4 GPa	4 GPa	5 GPa	
Longitudinal Tensile Stress	x_t	440 MPa	480	1900 MPa	
Longitudinal Compressive Stress	y_c	440 MPa	480	1900 MPa	Yield strength
Transverse Tensile Stress	x_c	425 MPa	190	1300 MPa	$\sigma_v=650$ MPa
Transverse Compressive Stress	y_c	425 MPa	190	1300 MPa	
Density	ρ	1900 kg/m ³	1400 kg/m ³	1900 kg/m ³	7700 kg/m ³

It is noteworthy that fixator connecting rod of stainless steel made in form of a hollow tube, and fixator connecting rod of composite material made in form of a full pipe, ie. The rod.

The fixator connecting rod that is made in combination E glass / epoxy has the worst mechanical properties compared with the other two tested composites. This is due to poor mechanical properties of E glass. As regards of E glass, it is the most commonly used fiber glass. E fiber glass has increased resistance to humidity and milder chemicals, but compared to Kevlar 49 and carbon fiber, has a significantly poorer mechanical properties.

Composite comprising a combination of aramid fibers, in the case of Kevlar 49 and the epoxy resin is a solution with better mechanical properties compared to the combination of E glass / epoxy. Lack of aramid fiber is water absorption. Kevlar fibers have a lower density of E glass, but on weight of fixator connecting rod, made from Kevlar fiber, affects the absorption of water and humidity, which can increase the weight of up to 7%.

The combination of carbon fiber and epoxy resin is one of the most quality solutions in terms of mechanical properties of composites. Unlike composites reinforced with E glass and aramid fibers, carbon fiber used in construction and mechanical parts that are exposed to greater loads. The best examples of such structures are the car's chassis, body and wings of aircraft etc. The lack of carbon fibers is their price, which is higher than the price of other fibers.

3. Stiffness analysis on axial compression

During the axial compression testing, the bone models were supported on ball joints, while maximal axial loading force applied to the proximal bone model was $F_p = 600$ N. The modeling of the influence of supports was performed using a Smooth virtual part. At the end of the proximal bone segment, the axial load in the form of surface force (Force density) was applied in the direction of the z axis of the Cartesian coordinate system.

A displacement constraint of the Sarafix FEM model was derived by using the Ball joint restraint on the model of distal bone segment. Likewise, a displacement constraint at the model of proximal bone segment was performed by using the User-defined restraint, which prevented the two translations in direction of x and y axis of the Cartesian coordinate system (Figure 2).

Figure 2 shows the 3D FEM model of the analyzed configuration Sarafix fixator (F50) before and after the action of maximum axial load. The directions and intensities of deformation of each point of the structure of the system and bone models are observed in the Figure 2.

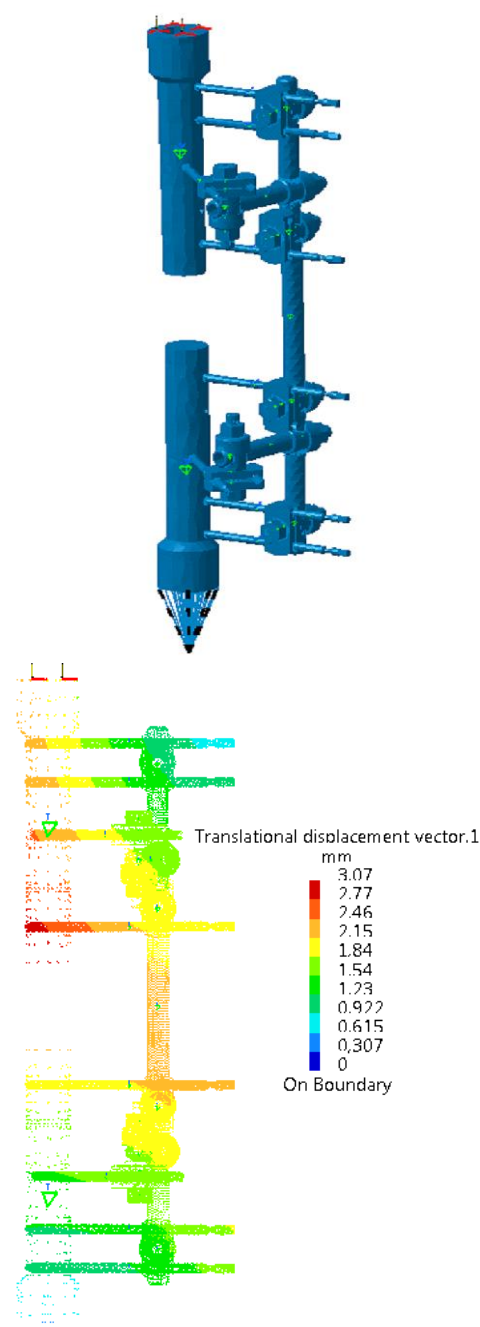


Fig. 2: Non-Deformed and Deformed Structure of the Sarafix (F50) Under Maximum Axial Load and Translation Displacement Vectors.

Diagram of axial displacement proximal segment model of bone at the point of load (Figure 3) was obtained by three analyzed Sarafix fixator configuration and C50 configuration. Figure 3 shows the intensity of deformation of the analyzed Sarafix fixator configuration and C50 configuration during testing under axial compression.

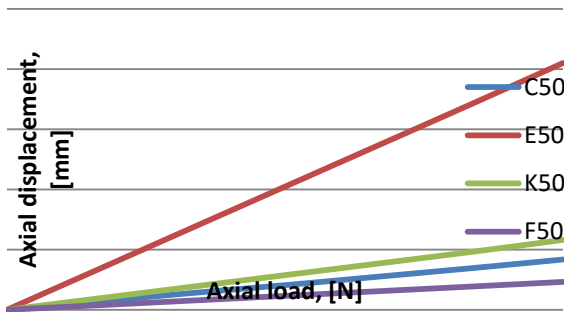


Fig. 3:Comparative Diagram of the Axial Displacement at the Point of Load.

Axial fixator stiffness (C_p) was calculated using the following equation:

$$C_p = \frac{F_p}{\delta_p} \text{ (N/mm)} \quad (1)$$

Where:

F_p – is the applied axial loading force (N),

δ_p – is the axial displacement of proximal segment at the point of load (mm).

The axial fracture stiffness was calculated as the applied axial force divided by total displacement at the analyzing points [5]:

$$C_{pp} = \frac{F_p}{R} = \frac{F_p}{\sqrt{(r_{D(x)})^2 + (r_{D(y)})^2 + (r_{D(z)})^2}} \quad (2)$$

4. Stiffness analysis on AP bending

During the testing under AP four-point bending (Fig. 4) models of the bones are free to rely on the cylinder with a flat surface reliance, while the maximum value of bending force was: $F_s = 500$ N.

The load was applied at the point of fracture on two half pins. In order to prevent the movement of the model in the space, the proximal bone model prevented the three translations, and the distal bonemodel prevented the two translations.

Figure 4 shows the 3D FEM model of the analyzed Sarafix fixator configuration F50 before and after the action of maximum bending force, which acts simultaneously on both models of bone segments.

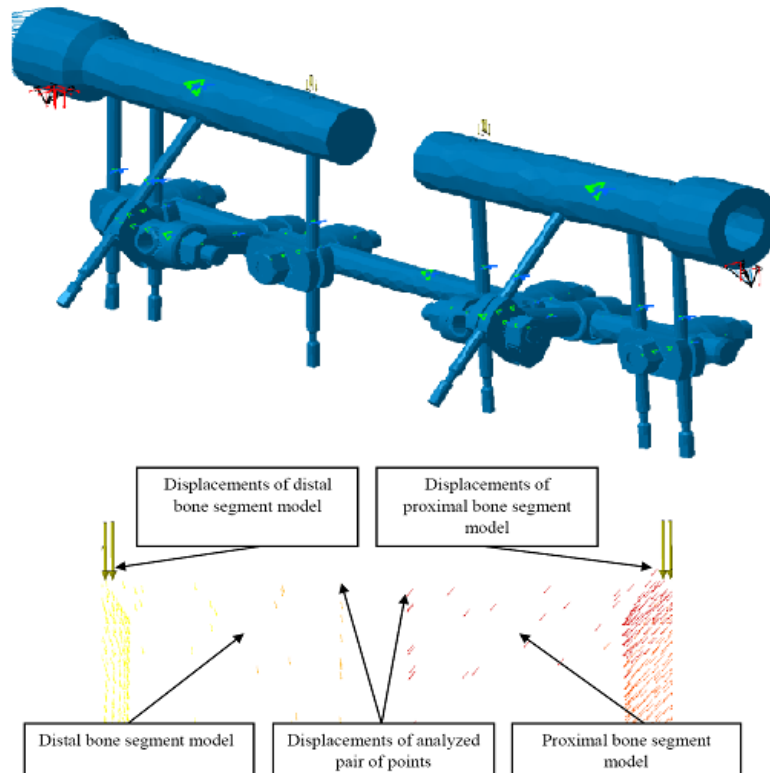


Fig. 4:Non-Deformed/Deformed Structure of the Sarafix Fixator (F50) and Translation Displacement Vectors at the Fracture Gap under Maximum Bending Force.

Directions and intensities of displacement of every point of the system structure and bone models are noted clearly.

AP bending fixator stiffness (C_s) determined as follows:

$$C_s = \frac{F_s}{\delta_s} \text{ (N/mm)} \quad (3)$$

Where:

F_s – Is the applied bending force (N)?

δ_s – is the displacement (deflection) of bone segment at the point of load (mm).

Diagram of the displacement proximal and distal segments of the bone models at the point of load (Figure 5) was obtained by three analyzed Sarafix fixator configuration and C50 configuration.

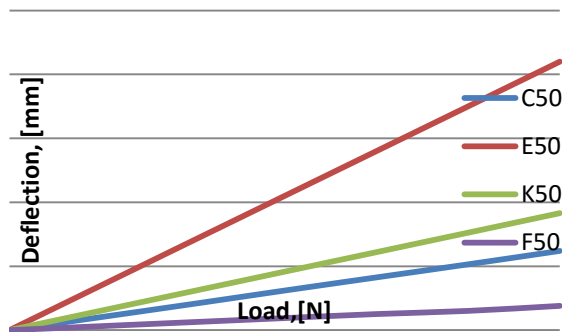


Fig. 5: Comparative Diagram of Deflection at the Point of Load.

The fracture bending stiffness was calculated as the applied bending force divided by total displacement at the analyzing points [5]:

$$C_{ps} = \frac{F_s}{R} = \frac{F_s}{\sqrt{(r_{D(x)})^2 + (r_{D(y)})^2 + (r_{D(z)})^2}} \quad (4)$$

5. Stiffness analysis on torsion

Testing under torsion was carried out by the principle of rotation distal segment of the bone model in relation to the fixed proximal segment. Torsion moment is defined on the hole surface in the segment of bone model. The maximum value of the torque was: $M_u = 15 \text{ Nm}$.

Figure 6 shows the 3D FEM model of the three Sarafix fixator configurations during structural analysis under torsion. Rotation of the system structure points after acting of the maximum torque is noted clearly.

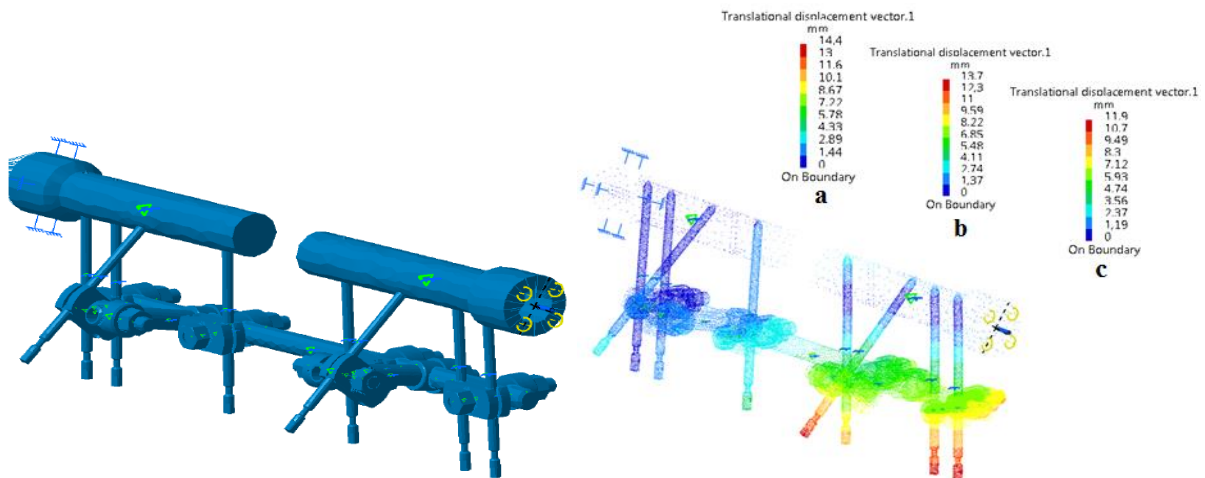


Fig. 6: Non-Deformed/Deformed Structure of the Sarafix Fixator and Translation Displacement Vectors Under Maximum Torque - (A) - Configuration E50, (B) - Configuration K50 and (C) - Configuration F50

Torsion fixator stiffness (C_u) is calculated using the following relation:

$$C_u = \frac{M_u}{\theta} \text{ (Nm/rad)} \quad (5)$$

Where:

M_u – is torque (Nm),

θ – is torsion angle of bone segment at the point of load (rad).

Using structural analysis, the diagram of torsion angle of proximal segment model of bone at the point of load was obtained (Fig. 7), which also shows the intensity of deformation of the three analyzed Sarafix fixator configuration and C50 configuration during testing under torsion.

The fracture torsion stiffness was calculated as the applied torque divided by total displacement at the analyzing points [5]:

$$C_{pu} = \frac{M_u}{R} = \frac{M_u}{\sqrt{(r_{D(x)})^2 + (r_{D(y)})^2 + (r_{D(z)})^2}} \quad (6)$$

6. Results

Values of displacement of proximal and distal model of the bone segment at the fracture gap under maximal axial load, bending force and torque are presented in Table 2.

Displacements were analyzed at the point of load and fracture gap using FEM. Based on the displacement at the point of load (δ i θ), the values of the fixator stiffness (C) are determined, based on the relative displacements at the fracture gap (R), the values of fracture stiffness (C_p) are determined as shown in the Table 2.

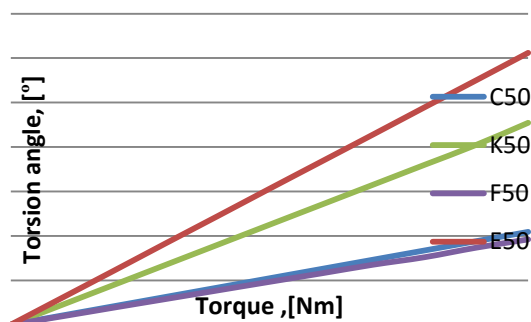


Fig. 7: Comparative Diagram of Torsion Angle at the Point of Load.

Table 2: Values of Stiffness and Displacements under Maximum Intensity of Loads

Type of load Construction	Displ. of the prox. segment at the fracture gap, mm			Displ. Of the distal. segment at the fracture gap, mm			Max. relat. displ. at the gap, mm	Displ. at the point of load, mm; rad*	Fracture-re stiff., N/mm; Nm/mm [#]	Fixator stiff., N/mm; Nm/rad [#]	
	D _{p(x)}	D _{p(y)}	D _{p(z)}	D _{d(x)}	D _{d(y)}	D _{d(z)}	R	δ; θ*	C _p	C	
Axial compression	E50	-4,06	24,3	-21	-1,36	29	1,77	23,4	20,5	25,64	29,26
	K50	-0,54	6,46	-5,74	-0,54	6,67	0,35	6,09	5,81	98,52	103,27
	F50	0,13	2,12	-2,22	0,16	2,22	0,094	2,31	2,32	289,64	258,62
AP bending	C50	0,53	4,14	-4,36	0,53	4,29	0,22	4,58	4,18	130,93	143,54
	E50	0,19	9,66	-6,94	0,32	8,01	1,34	8,44	7,17	59,24	69,73
	K50	0,24	2,66	-2,9	0,29	3,65	0,63	3,66	3,17	136,61	157,72
Torsion	F50	0,17	1,28	-0,22	0,21	1,28	0,54	0,76	1,14	657,69	438,59
	C50	-0,03	2,8	-0,53	-0,03	2,8	2,21	2,74	2,48	180,22	201,61
	E50	3,5	1,1	0,3	0,1	0,2	0,1	3,52	0,217*	4,26 [#]	69,12 [#]
	K50	2,2	0,56	0,1	0,06	0,04	0,01	2,2	0,158*	6,18 [#]	94,93 [#]
	F50	1,71	0,051	0	0,01	0	0	1,5	0,067*	8,82 [#]	223,87 [#]
	C50	0,82	0	0	0,05	0	0	0,76	0,073*	19,74 [#]	205,48 [#]

7. Conclusion

Optimal mechanical environment, which promotes bone healing, has not been completely defined yet. It is known that the directions and intensities of interfragmentary displacements in fracture gap, as well as stiffness of external fixator, affect the outcome and speed of the fractures' healing. Interfragmentary displacements parallel to the fracture surfaces, lead to the appearance of pseudo-arthritis instead of fracture healing. For these reasons, it is necessary to control interfragmentary displacements, especially to minimize transverse (shearing) displacements of bone ends at the fracture gap.

Using the developed FEM model of the Sarafix fixator, for each case load it is possible to track 3D displacement of any point of the bone-fixator system and interfragmentary displacements within the area of fracture. It is shown that the CATIA software system can be successfully used in the development of 3D geometrical models, FEM analysis and computer simulations of the process from different areas of technics and medicine.

Based on the results, it can be noticed that the configuration F50 has the highest stiffness, and the configuration E50 has the smallest stiffness, as expected, considering the material which is applied to the connecting rod in these two cases. Configuration E50 which is made of E glass has a 19.5% and 8.9% higher stiffness value to the stiffness of the configuration C50 and F50. The stiffness value of configuration K50 has the closest stiffness value of configuration C50, but not a proper substitute in case of load axial force.

In the case of testing under AP four-point bending, also the configuration F50 has the highest stiffness, and the configuration E50 has the smallest stiffness. Stiffness value (fracture and construct) of configuration F50 is significantly higher than stiffness value of configuration C50. It is noticeable that the stiffness value (fracture and construct) of configuration C50 has a 27% and 45% higher stiffness value to the stiffness of the configuration F50.

In the case of testing under torsion, configuration F50 has a 8% higher value of construct stiffness to the stiffness of the configuration C50, but significantly lower fracture stiffness by 56%. Based on the results of displacement and stiffness, in the case of testing under torsion, it is easy to conclude that the connecting rod made of stainless steel shows better mechanical performance compared to a connecting rod made of composite carbon fiber / epoxy resin. Fibers direction in relation to the load is the main reason why the results of configuration F50 inferior to the configuration C50. Torsion moment operates around the 'z' axis, which means that the shearing occurs in the transverse plane in which analyzed composite materials have poor mechanical properties than stainless steel.

For these reasons, from the aspect of stiffness, it can be concluded that an adequate substitution for the existing material which makes fixator Sarafix, represents a composite material based on carbon fiber and epoxy resin.

References

- [1] Mesic, E., Development of an integrated CAD/KBE system for design/redesign of external bone fixation devices, *University of Sarajevo, Faculty of Mechanical Engineering*. (2013).
- [2] Harris, B., Engineering Composites Materials, *the Institute of Materials*. London, GB, (1999).
- [3] Koo, T.K.K., Chao, E.Y.S., Mak, A.F.T., Fixation Stiffness of Dynafix Unilateral External Fixator in Neutral and Non-neutral Configurations, *Bio-Medical Materials and Engineering*, 15. pp. 433-444, (2005).
- [4] Radke, H., Aron, D.N., Applewhite, A., Zhang, G., *Biomechanical Analysis of Unilateral External Skeletal Fixators Combined with IM-Pin and without IM-Pin Using Finite-Element Method*, *Veterinary Surgery*, 35. pp. 15-23, (2006). <http://dx.doi.org/10.1111/j.1532-950X.2005.00106.x>.
- [5] Mesic, E., Research of Mechanical Stability of the Sarafix External Fixation System, University of Sarajevo, Faculty of Mechanical Engineering, (2008).
- [6] Fleming, B., Paley, D., Kristiansen, T., Pope, M., *A Biomechanical Analysis of the Ilizarov external fixator*, *ClinOrthop* 241:95, (1999).
- [7] Jasinska-Choromanska, D., Sadzynski, I., *Monitoring Technique of Bone Fracture Healing Using External Fixators*, 39th International Conference, Experimental Stress Analysis, pp. 35-40, (2001).
- [8] Mesic, E., Pervan, N.; Repcic, N. & Muminovic, A., Research of Influential Constructional Parameters on the Stability of the Fixator Sarafix, *Annals of DAAAM for 2012 & Proceedings of the 23rd International DAAAM Symposium*, ISBN 978-3-901509-91-9. ISSN 2304-1382. pp 0561 – 0564. Vienna, Austria, (2012).
- [9] <http://www.performance-composites.com/>. Lastvisit 22.04.2014.
- [10] Thakurdesai PA, Kole PL & Pareek RP (2004), Evaluation of the quality and contents of diabetes mellitus patient education on Internet. *Patient Education and Counseling* 53, 309–313. <http://dx.doi.org/10.1016/j.pec.2003.04.001>.
- [11] Mešić, E., Avdić, V., Pervan, N.: *Numerical and experimental stress analysis of an external fixation system*, *Folia Medica, Facultatis Medicinae Universitatis Saraevensis*, Vol.50, No.1.: 74-80, (2015).
- [12] Mešić, E., Avdić, V., Pervan, N., Repčić, N.: *Finite Element Analysis and Experimental Testing of Stiffness of the Sarafix External Fixator*, 25th DAAAM World Symposium „Intelligent Manufacturing & Automation 2014“.